applied sciences

MDPI

Article

The Neotectonic Deformation of the Eastern Rif Foreland (Morocco): New Insights from Morphostructural Analysis

Mohamed Makkaoui [1], Omar Azzouz [1], Víctor Tendero-Salmeron [2], Kamal Belhadj [1] and Jesus Galindo-Zaldivar [3,*]

[1] Laboratoire de Géologie Appliquée, Faculté des Sciences, Université Mohammed Ier, Oujda 60000, Morocco; makkaoui_mohamed1718@ump.ac.ma (M.M.); azzouzomar@yahoo.fr (O.A.); belhadj.kamal@gmail.com (K.B.)
[2] Instituto de Ciencias del Mar (ICM)—CSIC, 08003 Barcelona, Spain; vtendero@ugr.es
[3] Departamento de Geodinámica, Universidad de Granada, 18071 Granada, Spain
* Correspondence: jgalindo@ugr.es

Abstract: The Rif Cordillera, an Alpine orogen in the Western Mediterranean, was developed by the interaction of Eurasian and African (Nubia) plates. Neotectonic deformations of the Rif foreland influence the relief, especially in post-nappe basins and their boundaries with Jurassic and Cretaceous carbonate mountain massifs, and they contribute to highlighting the recent evolution of the Cordillera. The topographic and hydrological lineaments of these basins were characterised on the basis of multi-scale morphostructural data analysis, supported by digital mapping and GIS. They were correlated with geological structures, essentially with fractures. The outcrops of the Upper Tortonian and Messinian deposits depict well-defined geometric shapes with roughly rectilinear boundaries, as defined by their contacts with the massive and rigid rocks of the Jurassic and Cretaceous series. Upper Tortonian deposits evidence major regional N70°E and N40°E lineaments, which are obliquely intersected by late structures. Messinian N120°E and N25°E lineaments, associated with N140°E lineaments, are also recognised. The interpretation of these lineaments as faults indicates the activity of two systems of transtensive sinistral and then dextral brittle shearing that correspond to two episodes of neotectonic deformation that played a decisive role in shaping the reliefs of the Eastern Rif. These deformations are particularly relevant to isolate basins and likely have a key role during the closure of the South Rifian corridor during the Mediterranean Messinian Salinity crisis.

Keywords: morphostructural lineament analysis; neotectonic deformations; Eastern Rif; post-nappe basins; Morocco; Tortonian; Messinian

Citation: Makkaoui, M.; Azzouz, O.; Tendero-Salmeron, V.; Belhadj, K.; Galindo-Zaldivar, J. The Neotectonic Deformation of the Eastern Rif Foreland (Morocco): New Insights from Morphostructural Analysis. *Appl. Sci.* **2024**, *14*, 4134. https://doi.org/10.3390/app14104134

Academic Editor: Fabrizio Balsamo

Received: 20 February 2024
Revised: 1 May 2024
Accepted: 8 May 2024
Published: 13 May 2024

1. Introduction

Morphostructural analyses determine the imprint of tectonics in the relief to reveal the recent evolution of the deformation [1,2]. They contribute to unravelling the complex geological history and have applications in investigations of geological resources and hazards. The analysis of relief features of slopes, such as mountain fronts and fluvial networks, reveals linear features in some regions that may be associated with main brittle structures [3,4].

The Rif Cordillera (Figure 1) is part of the Alpine orogen in the Western Mediterranean [5,6], affected by several deformation phases that have produced folding and thrusting since the Oligocene. They deform the internal to external parts of the chain [7–9]. This compressional tectonic activity related to the oblique convergence of Africa (Nubia) and Eurasian plates (Figure 1a) is relayed in the Rif from the Late Miocene, when uplift and a decrease in deformation occurred [10–13]. Neotectonic deformations are not highly pronounced in post-nappe Neogene–Quaternary sedimentary basins, making them challenging to distinguish from earlier, intense Alpine deformation structures within the basement massifs. In fact, this is particularly evident in the opening of post-nappe basins

that develop along the southern edge of the chain (Figure 1b), where they form the South Rifian corridor, as well as in the basins along the Mediterranean coast associated with the opening of the Alboran Sea. Although previous research has improved our knowledge of the paleo-stress and neotectonic evolution that are considered in this region since the Late Miocene [11,14–17], to date, the morphostructure of the region has not been analysed in detail.

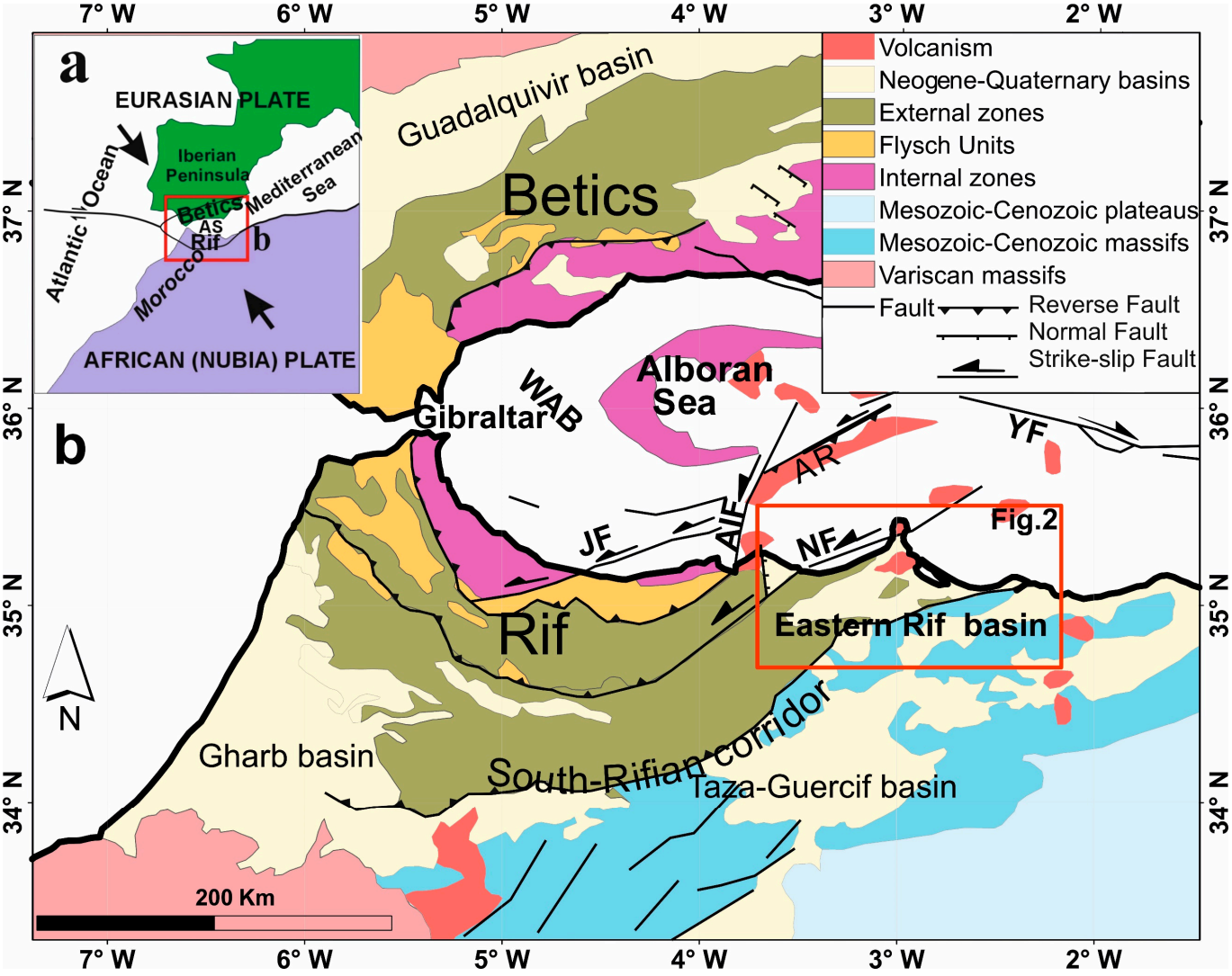

Figure 1. Structural sketch of plate boundaries (**a**) and of the Betic Rif Cordillera (**b**). Modified from [18]. Arrows in Figure 1a indicate the plate convergence. The detailed study area of Figure 2 is indicated. AIF, Al Idrissi Fault; AR, Alboran Ridge; AS, Alboran Sea; JF, Jebha Fault; NF, Nekor Fault; YF, Yusuf Fault; WAB, Western Alboran Basin.

Sedimentary basins are mainly filled by Upper Miocene detritic deposits represented mainly by formations of the Upper Tortonian and Messinian, overlaid by scattered levels of Pliocene and Quaternary sediments. During the Messinian evolution, the closing of the Atlantic and Mediterranean connection along the South Rifian corridor due to tectonic evolution was a key process that finally developed the Messinian Salinity Crisis in the Mediterranean [19]. Moreover, some volcanism also occurred in this area. Basin boundaries are generally characterised by well-determined rectilinear contacts that produce geometric forms and occupy low areas framed by Jurassic and Cretaceous massifs (Figure 2). This geometry suggests that their individualisation is controlled by regional tectonic structures that played a decisive role in shaping morphostructural reliefs. Moreover, in sedimentary

basins, where marly sediments predominate, tectonic markers are scarce and often subject to complex reactivations and crosscuts. In this setting, morphostructural studies based on the characterisation of the main lineaments constitute a main tool that reveals the fracture pattern and contributes to highlighting the geodynamic processes.

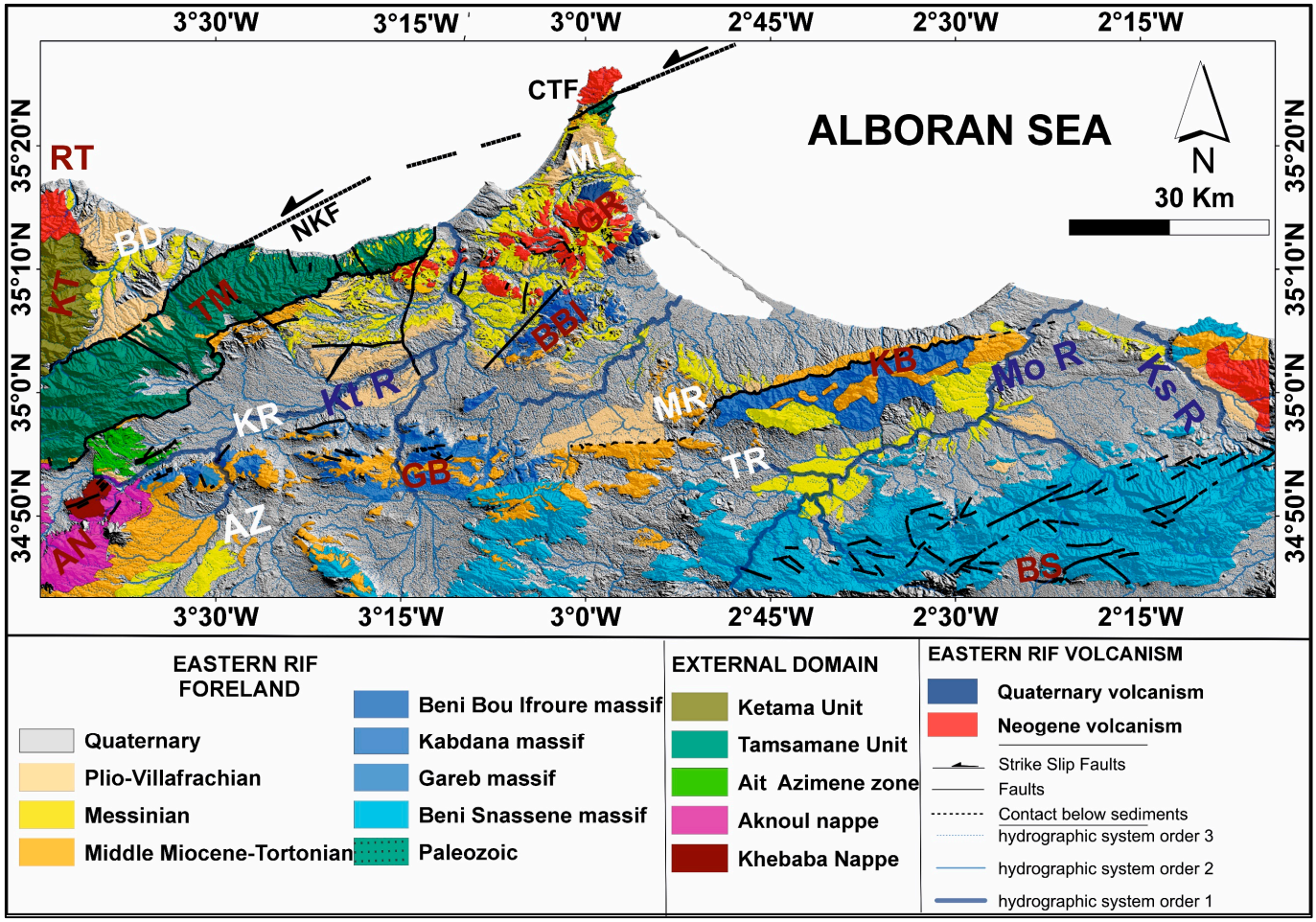

Figure 2. Synthetic geological map of the Eastern Rif that constitutes the study area. Modified from [20–32]. Massifs: AN, Aknoul Nappe; AZ, Ain Zora; BBI, Beni Bou Ifroure; BS, Beni Snassene; CTF, Cap des Trois Fourches; GB, Gareb; GR, Gourougou; KB, Kabdana; KT, Ketama; RT, Ras Tarf; TM, Tamsamane. Basins: BD, Boudinar; KR, Kert; ML, Melilla; MR, Moulay Rachid; TR, Triffa. Hydrographic network: Kt R, Kert River; Ks R, Kiss River; MoR, Moulouya River. Faults: NKF, Nekor Fault.

The aim of this contribution is to analyse the post-nappe deformations of the Eastern Rif by studying the neotectonic lineament patterns that reveal the tectonic structures controlling the shape of compartmentalised reliefs. We apply an approach that combines geological data and morphostructural analysis, supported by digital mapping, to characterise and analyse the regional lineaments presented by the major massifs and rivers that cross the area. Additionally, on a local scale, we examine the lineaments determined by the smaller mountains within each massif and small rivers. The information provided by the patterns of morphological lineaments is related to brittle deformations and evaluated to improve the knowledge of the geological evolution of the Eastern Rif in the framework of the Eurasian–African (Nubia) convergence (Figure 1a).

2. Geological and Tectonic Context

The Rif Cordillera belongs to the Tethys Alpine Orogenic Belt and together with the Betic Cordillera constitutes an arcuate orocline, which meets at Gibraltar and surrounds the Alboran Sea. The Rif is formed by three structural elements belonging to different paleogeographic domains [10,33,34] (Figure 1b), namely the following:

- Internal zones, also called the Alboran Domain, correspond to an ancient continent that exists off Africa, in the western Tethys. It consists of a turn of three tectonic complexes: the Sebtides, Ghomarides, and the Calcareous Dorsal [10,35].
- Flysch units that develop on transform zones between the Afro-European margins and the Alboran Domain; these flysches are grouped into two stratigraphic units, one Mauritanian and the other Massylian [36,37]. The Mauritanian flysch includes the Tisirene flysch, of the Late Jurassic–Early Cretaceous age, and the Beni Ider flysch, of the Middle Paleogene–Burdigalian age. The Massylian flysch includes the Early Cretaceous and Numidian flysch of Paleogene–Burdigalian age [38].
- External zones, which represent the Tethyan margin of the African plate; this domain consists mainly of terminal Cretaceous parautochthonous terrains represented by the Tangier–Loukous units and Triassic–Tertiary parautochthonous-to-autochthonous carbonate and siliciclastic terrains represented by Mesorifain and pre-Sahelian units [38,39].

In the Eastern Rif, the Mesorifain units of Tamsamane are directly in contact with the foreland. Thus, the internal foreland has a Rifian affinity, whose Mesozoic formations show stratigraphic and metamorphic similarities with Mesorifain formations, such as the massifs of Kabdana, Beni Bou Ifroure, Gareb, and Cap des Trois Fourches (Figure 2) [8,40–42]. In contrast, their equivalent of the Outer foreland is the Beni Snassene Massif, without Alpine metamorphism, which is shown with the highlands, Atlasic affinities (Figure 2) [43–45].

These Mesozoic series outcrop only at the level of the reliefs where they are unconformably overlaid by deposits of the Lower and Middle Miocene and form isolated mountain massifs that emerge in the regional topography [12,46,47]. These geological formations are shown here as a relative para-substratum surmounted by a complex arrangement of lowland plains occupied by Upper Miocene formations considered as post-nappe deposits [48,49]. The shape of these contrasting and compartmentalised structures is clearly related to neotectonic deformations [50].

The post-nappe basins infill starts with a thick series of Tortonian conglomerates and marls that only outcrop at the foot of the mountain ranges and show significant lateral variations in thickness [17,48]. Indeed, these formations are differently distributed and are partially cached below the Messinian marls and finally the Pliocene–Quaternary detrital deposits. Their development occurred in isolated basins induced by subsidence phenomena controlled by brittle deformations.

3. Materials and Methods

3.1. Elaboration of the Synthetic Geological Map of the Eastern Rif

The elaboration of a synthetic geological map of the Eastern Rif (Figure 2) is based on the one hand on the set of geological data recovered from 13 geological maps (Figure 3), including 10 maps at 1:50,000 for sheets of Nador [20], Melilla [21], Zegangane [22], Kebdani [23], Boudinar [24], Midar [25], Ain Zohra [26], Ahfir [27], Berkane [28], and Zaio [29]; a map at 1:100,000 for the leaves of Tiztoutine [30]; and 2 maps at 1:500,000 for the sheets of Oujda [31] and the Rif [32]. Secondly, it is based on the many studies that were conducted in the research area, including the studies of [7,10,51–55].

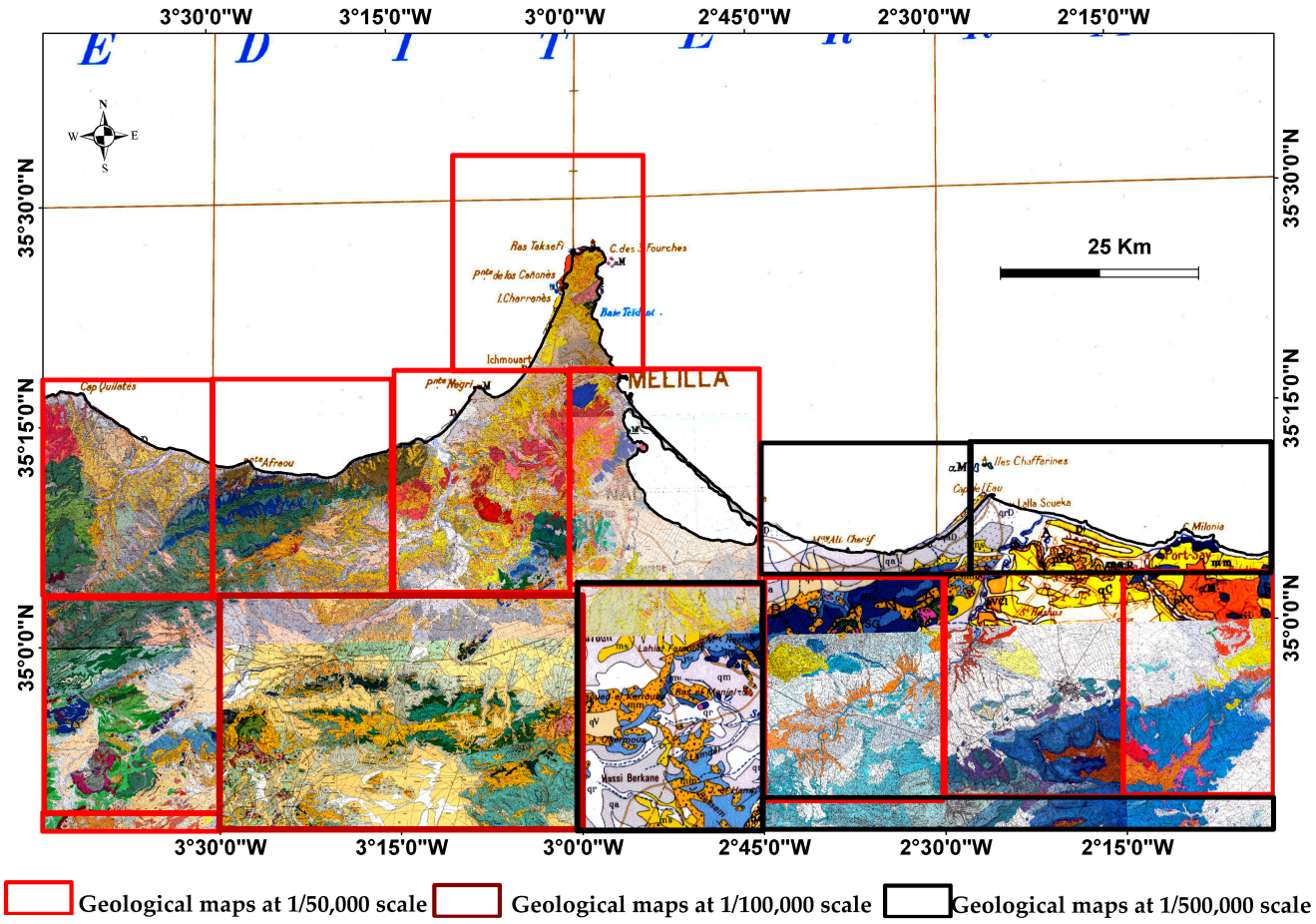

Figure 3. Compilation of geological maps used in the elaboration of the synthetic geological map of the Eastern Rif. Sources are indicated in the text.

3.2. Extraction of Lineaments

Lineaments of the Eastern Rif were extracted (Figure 4) from the morphostructural analysis of three main sources: (1) Digital mapping was conducted using 24 topographic maps at 1:50,000 scale, which cover the study area (Figure 5). (2) DEM images were processed using a shading tool based on the method outlined by [56–60]. These DEMs have a resolution of 12 m and can be downloaded from the website referred to in Figure 5. (3) Satellite images from Google Earth (https://www.google.com/intl/es/earth/ accesed on 30 January 2024), and ArcGIS Earth (version 1.9.2351) were also used.

We used qualitative interpretation of aerial images and digital terrain data (DEM, Figure 5) to map the lineaments within the Eastern Rif area. Roughly linear features are represented by straight lineaments, following the common practice of interpreting geological attributes such as bedding and fracture traces. This process involved manual tracing of lineaments, which proved highly beneficial for studying tectonic structures. We considered various geomorphological features like ridge lineaments and drainage patterns when mapping these lineaments. The y outlines the ridge linear features visible in hillshade relief maps (Figure 6). Additionally, they reveal straight segments within the stream networks, as depicted in hydrographic maps (Figure 7). This meticulous approach ensures accurate mapping of mountain boundaries.

The results of the qualitative interpretation of these lineaments are presented on the background of reliefs (Figure 8) obtained by the treatment of DEM shadows.

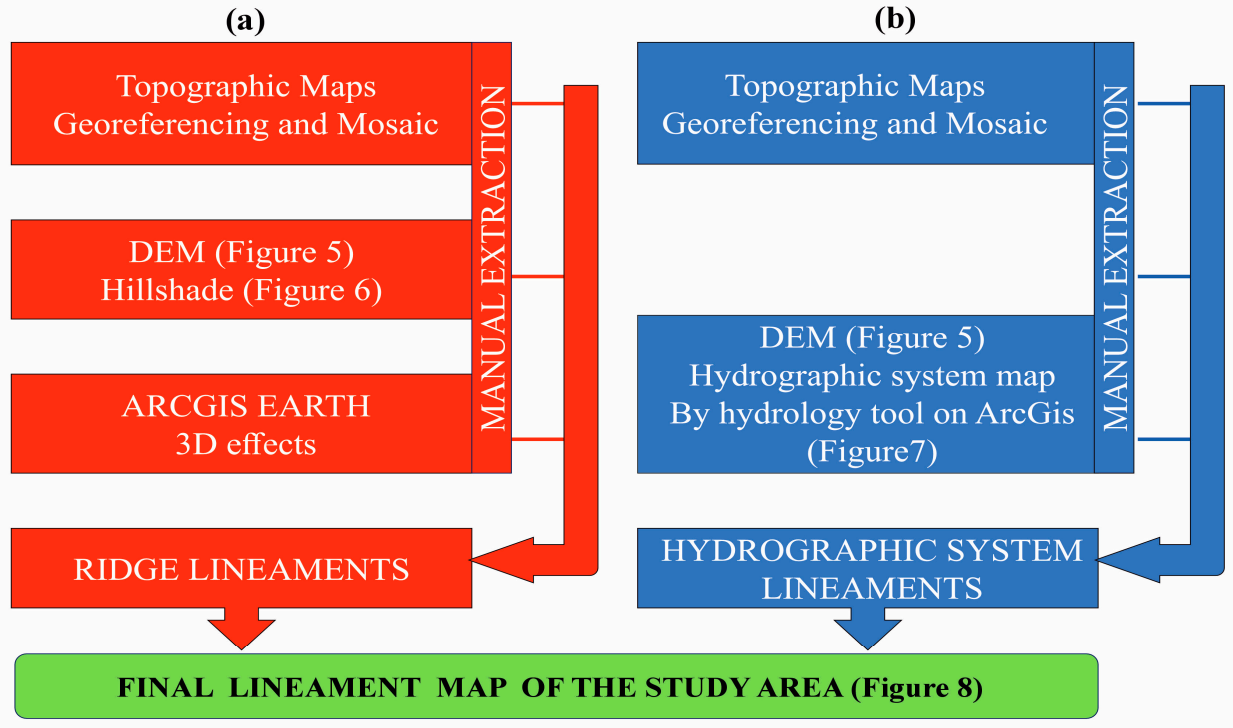

Figure 4. Flowchart of the methodology adopted for tracing the structural lineaments: (**a**) for ridge lineaments and (**b**) for hydrographic network lineaments.

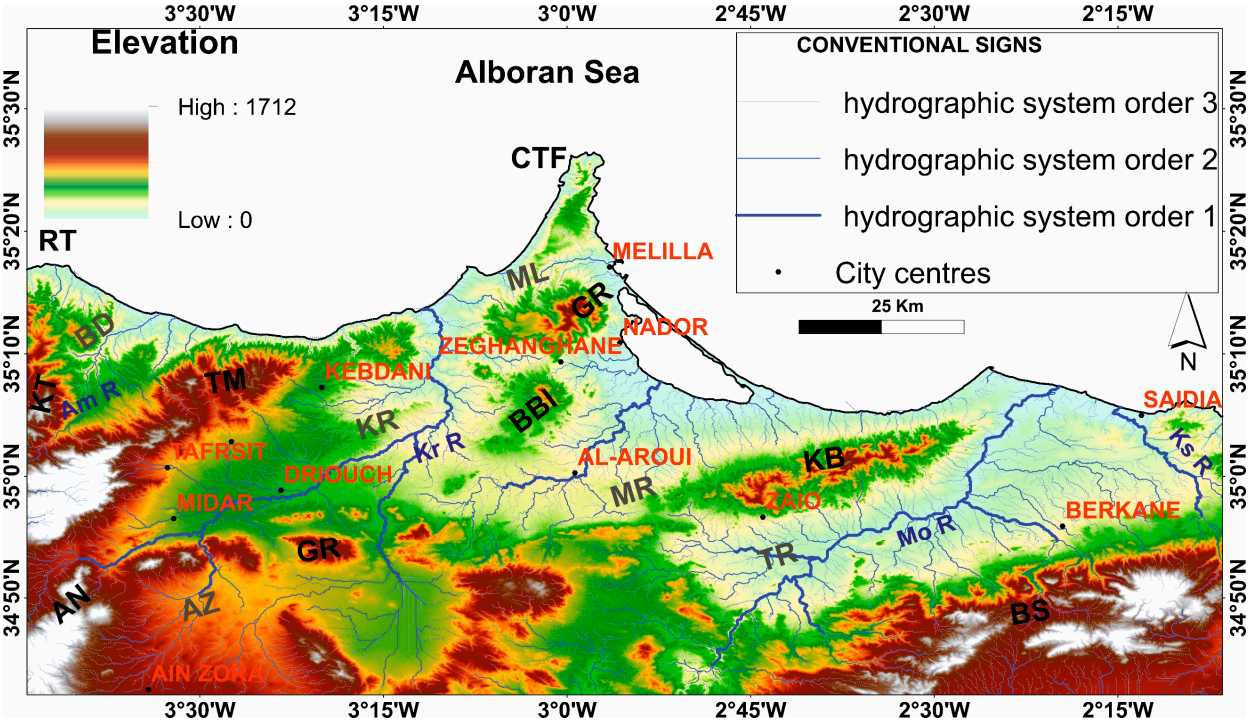

Figure 5. DEM image of Eastern Rif (https://asf.alaska.edu/datasets/daac/alos-palsar/ accesed on 20 January 2024). Massifs: AN, Aknoul Nappe; AZ, Ain Zora; BBI, Beni Bou Ifroure; BS, Beni Snassene; CTF, Cap des Trois Fourches; GB, Gareb; GR, Gourougou; KB, Kabdana; KT, Ketama; RT, Ras Tarf; TM, Tamsamane. Basins: BD, Boudinar; KR, Kert; ML, Melilla; MR, Moulay Rachid; TR, Triffa. Hydrographic network: Am R, Amakran River; Ks R, Kiss River; Kt R, Kert River; MoR, Moulouya River.

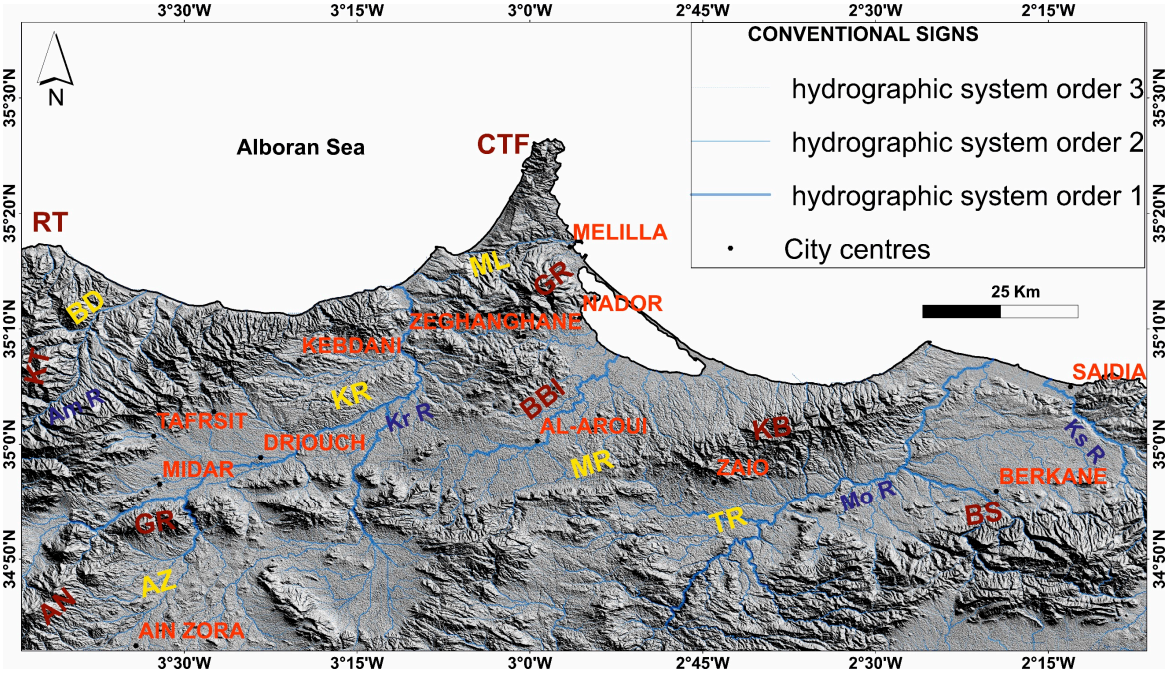

Figure 6. Topography of the Eastern Rif (digital processing of DEM (Figure 5) by hillshade). Massifs: AN, Aknoul Nappe; AZ, Ain Zora; BBI, Beni Bou Ifroure; BS, Beni Snassene; CTF, Cap des Trois Fourches; GB, Gareb; GR, Gourougou; KB, Kabdana; KT, Ketama; RT, Ras Tarf; TM, Tamsamane. Basins: BD, Boudinar; KR, Kert; ML, Melilla; MR, Moulay Rachid; TR, Triffa. Hydrographic network: Am R, Amakran River; Ks R, Kiss Rive; Kt R, Kert River; MoR, Moulouya River.

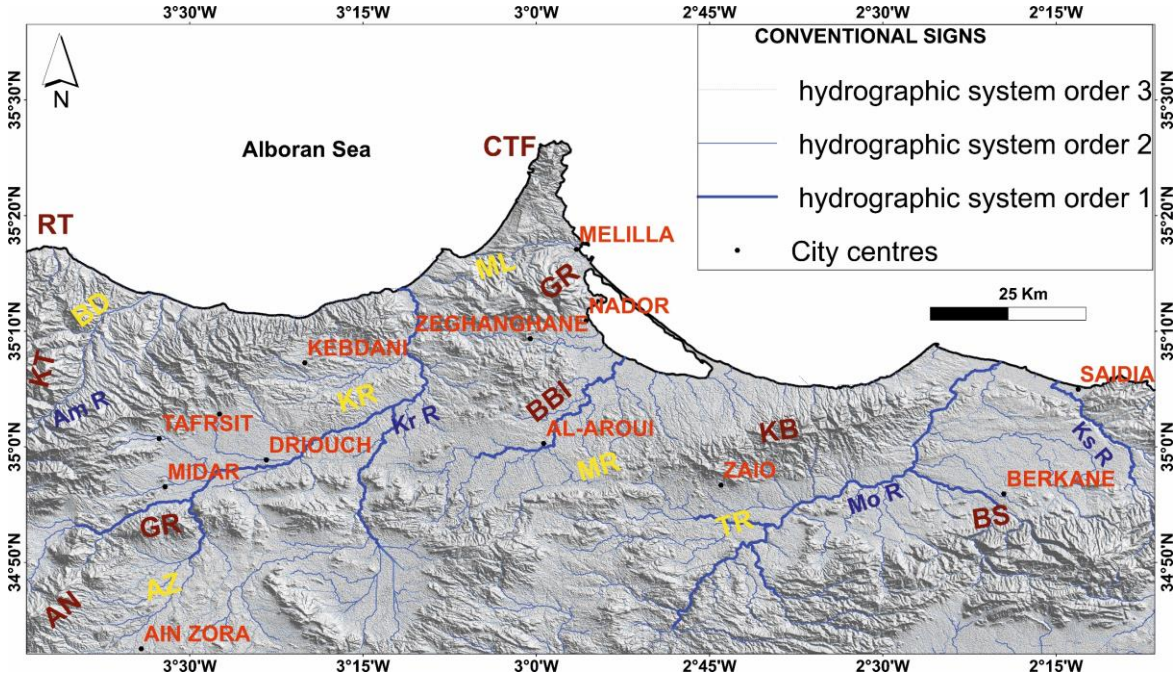

Figure 7. Hydrographic network map of the Eastern Rif. Massifs: AN, Aknoul Nappe; AZ, Ain Zora; BBI, Beni Bou Ifroure; BS, Beni Snassene; CTF, Cap des Trois Fourches; GB, Gareb; GR, Gourougou; KB, Kabdana; KT, Ketama; RT, Ras Tarf; TM, Tamsamane. Basins: BD, Boudinar; KR, Kert; ML, Melilla; MR, Moulay Rachid; TR, Triffa. Hydrographic network: Am R, Amakran River; Ks R, Kiss River; Kt R, Kert River; MoR, Moulouya River.

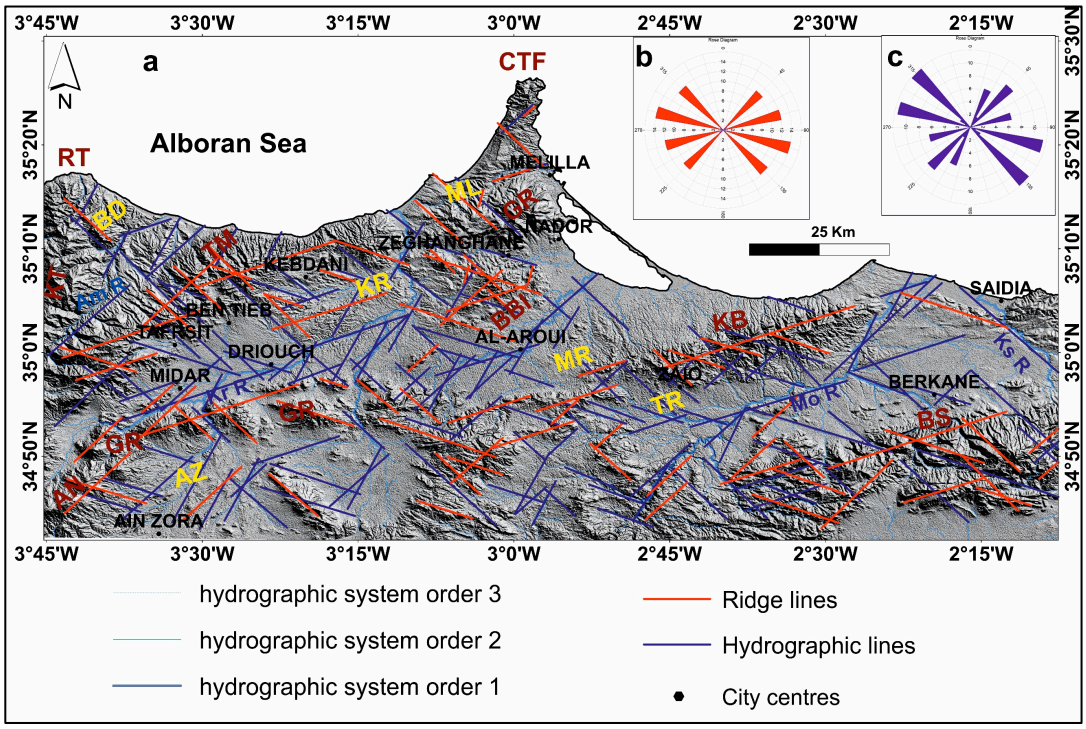

Figure 8. Eastern Rif lineament map (**a**) with the rose diagrams of crest lineaments (**b**) and hydrographic lineaments (**c**). Massifs: AN, Aknoul Nappe; AZ, Ain Zora; BBI, Beni Bou Ifroure; BS, Beni Snassene; CTF, Cap des Trois Fourches; GB, Gareb; GR, Gourougou; KB, Kabdana; KT, Ketama; RT, Ras Tarf; TM, Tamsamane. Basins: BD, Boudinar; KR, Kert; ML, Melilla; MR, Moulay Rachid; TR, Triffa. Hydrographic network: Am R, Amakran River; Ks R, Kiss River; Kt R, Kert River; MoR, Moulouya River.

3.2.1. Ridge Lineament Extraction

The manual extraction of ridge lineaments (Figure 4a) was performed based on data obtained from the analysis of topographic maps and processing of shading maps (Figure 6), utilising 'Hillshade', a tool within the 3D analysis suite of ArcGIS. These ridge features were cross-referenced with relief images acquired using 'ArcGIS Earth'.

3.2.2. Hydrographic Lineament Extraction

The manual extraction of hydrographic lineaments (Figure 4b) was carried out on the basis of consistency between hydrographic network delineations provided by topographic maps and those automatically extracted by the hydrology tool in 'spatial analyst tools' under 'ArcGIS' following the steps of this tool (Flow Direction, Flow Accumulation, and Stream Order). In addition, we took into account the average irregularities of these features, which were defined by the order and extent of their branches at both local and regional scales (Figure 7).

3.3. Morphostructural Analysis

The predominance of soft facies occupying the study area hides the presence of adequate outcrops for field observation of tectonic structures. This is one of the main issues in revealing the geodynamic space-time processes of neotectonic deformations that controlled the individualisation of different Neogene basins of the Eastern Rif.

To address this issue, the morphological markers induced at the surface by this neotectonic activity produced regional lineaments that represent linear features in a landscape and are related to geological structures. They evidenced the alignment of the major mountain ranges and rivers within the study area, as well as small-scale lineaments associated with

the small mountains within each range. These lineaments are identified by qualitative photo interpretation of aerial images and DEM, following the procedure outlined in Figure 4.

3.3.1. Ridge Lineament Analysis

In this analytical approach, morphostructural analysis focuses on the fact that ridge lineaments defined by mountain massifs are considered markers that indicate the layout and extensions of tectonic compartments in elevated positions, framed by collapse faults. The ridge lineaments are evidenced by the contrasting morphological characteristics due to the resistant nature of carbonate mountain massifs, in contrast to the predominant post-nappe detrital and marly soft deposits in the plains (Figure 2). The major ridges exhibit greater prominence and are delineated on a regional scale by the segmented and elongated shapes of mountain massifs such as the Beni Snassen massif, Kebdana, Beni Bou Ifroure, Gareb, Tamsamane and Cap des Trois Fourches (Figures 6 and 8). In addition, the minor ridge lineaments correspond to the mountains within each massif. The analysis of ridge and massif boundaries reveals the behaviour of the tectonic blocks.

3.3.2. Hydrographic Lineament Analysis

The morphostructural analysis of hydrographic lineaments focuses on the idea that they emerge along zones of lower relief, which have undergone the maximum amount of collapse and erosion, coinciding primarily with fractures that have influenced the shaping of the morphostructural features of the Eastern Rif. In general, the hydrographic network is controlled by two major parameters: slope and tectonics [1,2]. It is estimated that the Eastern Rif is characterised in the majority by reliefs of low slopes that correspond to the post-nappe basin. The region is crossed by three large rivers (wadis, oueds): the Moulouya River at the Triffa Basin, the Kert River at the Kert Basin, and the Amakran River, which crosses the Boudinar Basin (Figure 7). These rivers intersect the middle part of the basins and flow towards the Mediterranean.

3.4. Separation of Tectonic Episodes

The lineament map (Figure 8) highlights the straight geometry of the Tortonian deposits, which are mapped along the margins of the ancient massifs (Figure 2), as well as the boundaries of the Messinian geological formations (Figure 2). The interpretation of fractures is supported by geological maps (Figures 2 and 3) derived from field data and aerial images from Google Earth and ArcGIS Earth. The geometry of the contacts and the kinematics of certain faults, as determined by the displacement of markers, contribute to distinguishing between the tectonic episodes that governed the activity of the faults during Tortonian and Messinian sedimentation and deducing the behaviour of the fault system during each episode.

4. Results

The study area corresponds to the northeastern part of the Rif Cordillera. It spreads between the massif of Ras Tarf in the west and River Kiss in the east (Figures 1 and 2). This sector is mainly occupied by low-relief plains (Figure 5) of marly facies post-nappe deposits (Figure 2) and by mountainous massifs that have delimited the Neogene basins in the northern part of the Rif corridor (Figure 2).

4.1. Morphostructural Analysis

Contacts between mountain ranges and post-nappe basins in the Eastern Rif (Figures 2 and 8) are segmented and have well-defined orientations. This is clear for the Upper Tortonian and Messinian formations, which are predominantly marly facies, whose outcrops also arise in rhomboidal geometric shapes. Moreover, the rheological features of the massive and rigid materials of their Jurassic and Cretaceous carbonate basements played a decisive role in the structural reliefs of the Eastern Rif. The orientations of the main hydrographic network and the coastlines largely follow those of regional tectonic

structures, which produce uplift and subsidence, whereas the ridge lineaments correspond to the geometric attitude of the blocks and tectonic compartments.

4.1.1. Ridge Lineaments

The most important and expressive lineaments are delineated on a regional scale by the segmented, elongated shapes of the carbonate massifs located in the horst positions (Figure 8). They incorporate the highest elevations of various mountains that are oriented N70°E (Kabdana, Tamsamane, Gareb ouest, and Beni Snassene), N40°E (Beni Bou Ifroure, Tiztoutine), and N110°E (Gareb ouest and Beni Snassene) (Figure 8b). Additionally, other shorter ridge lineaments can be distinguished, defined on a local scale by the configuration of mountains within each carbonate massif. These partly follow orientations N70°E and N40°E; nevertheless, locally, oblique lineaments can be distinguished that are arranged along orientations ranging from N120°E to N135°E (Figure 8a).

4.1.2. Hydrographic Network Lineaments

Cartographic analysis shows that the plots of the Eastern Rif hydrographic network are organised according to well-defined orientations and lengths and can be grouped into two types. The difference between the two types of hydrographic networks was determined by the topographical features induced by the relative behaviour of the blocks, associated with the contrasting and compartmentalised structures of the thick, rigid Jurassic and Cretaceous carbonate series.

The first group crosses the mountainous massifs and is a very embedded hydrographic network, with a limited extension of orientations N70°E, N100°E, and N40°E (Figure 8c). Hydrographic networks in those areas are also related to the ridge lineaments, conditioned by the brittle deformation of their Jurassic–Cretaceous rigid rocks, marked by a partial stacking of tectonic packages due to fold and thrust structures.

The other group occupies low-lying areas of the post-nappe basins, which are predominantly marly. These areas concentrate in the hydrographic network. This is the case in the Kert, Gareb, and Triffa basins. These regional hydrographic networks often connect to such large tributaries N120°E to N140°E that cross the Kert Basin, as well as other more abundant tributaries and smaller extensions of orientations N25°E, sometimes N40°E.

4.2. Separation of Tectonic Episodes

4.2.1. Tortonian Episode

The first system of these neotectonic structures (Figures 9 and 10) is defined by the orientation of the mountain ranges of Kabdana, Gareb, Beni Bou Ifroure, Cap des Trois Fourches, and Tamsamane. These massifs stand on a large scale as regional tectonic packages that stand out in the regional topography caused by resistant rocks delimited mainly by tectonic structures [61,62]. The summits of the different mountains determine, on a large scale, lineaments of major ridges, of which the orientations N70°E and N40°E are established according to those of their geometric limits with the post-nappe basins (Figure 9).

The main Eastern Rif hydrographic network uses the low reliefs of the intermediate parts of the post-nappe basins. These major networks extend over tens of kilometres and have a segmented appearance that largely follows the N40°E and N70°E guidelines (Figure 9c). We consider their plots to coincide with the alignment of the maximum collapse zones induced by the basement contact with the Jurassic and Cretaceous carbonate series (Figure 2). We interpret them to be controlled in depth by the same N40°E and N70°E families of major fractures of the structures bounding the reliefs that developed complex structures in horsts and grabens (Figure 9c).

Moreover, the cartographic examination shows that these massifs present other lineaments of local peaks and kilometric extensions, defined at a smaller scale by the pattern of the different mountains and which are consistent with the orientations of the major ridge lineaments (Figure 9b). These observations allow us to associate N40°E and N70°E

structures with the first episode of brittle deformations of the Late Miocene that controlled the regional morphostructural shaping of the Eastern Rif foreland.

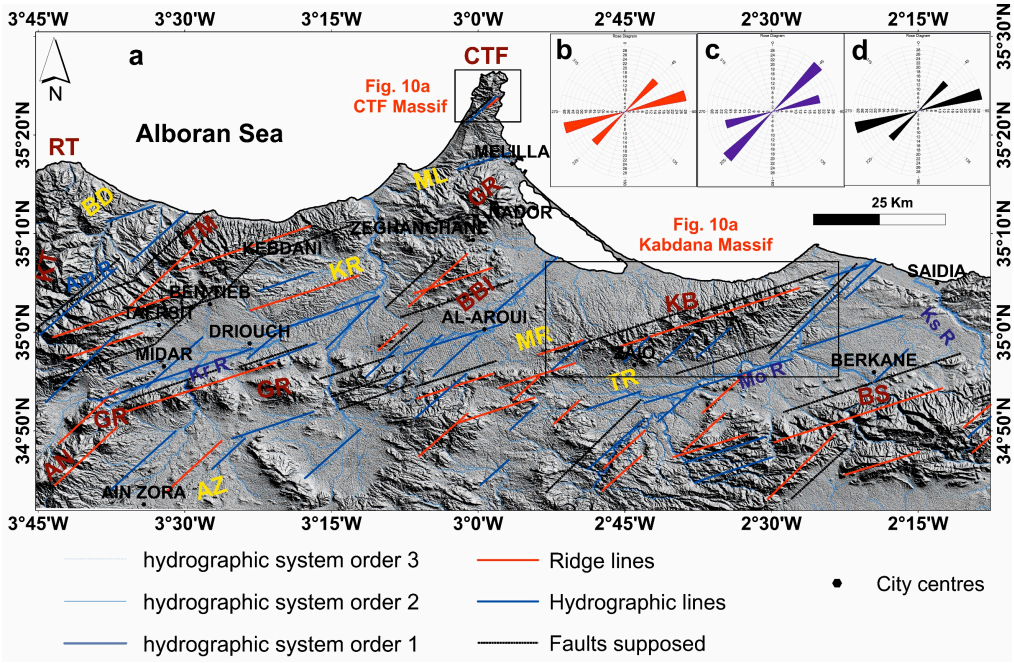

Figure 9. Lineament map (**a**) showing the major structure characterising the Tortonian deformation system: (**b**) rose diagrams of ridge lineaments, (**c**) rose diagrams of hydrographic lineaments, and (**d**) rose diagrams of supposed faults. Massifs: AN, Aknoul Nappe; AZ, Ain Zora; BBI, Beni Bou Ifroure; BS, Beni Snassene; CTF, Cap des Trois Fourches; GB, Gareb; GR, Gourougou; KB, Kabdana; KT, Ketama; RT, Ras Tarf; TM, Tamsamane. Basins: BD, Boudinar; KR, Kert; ML, Melilla; MR, Moulay Rachid; TR, Triffa. Hydrographic network: Am R, Amakran River; Ks R, Kiss River; Kt R, Kert River; MoR, Moulouya River.

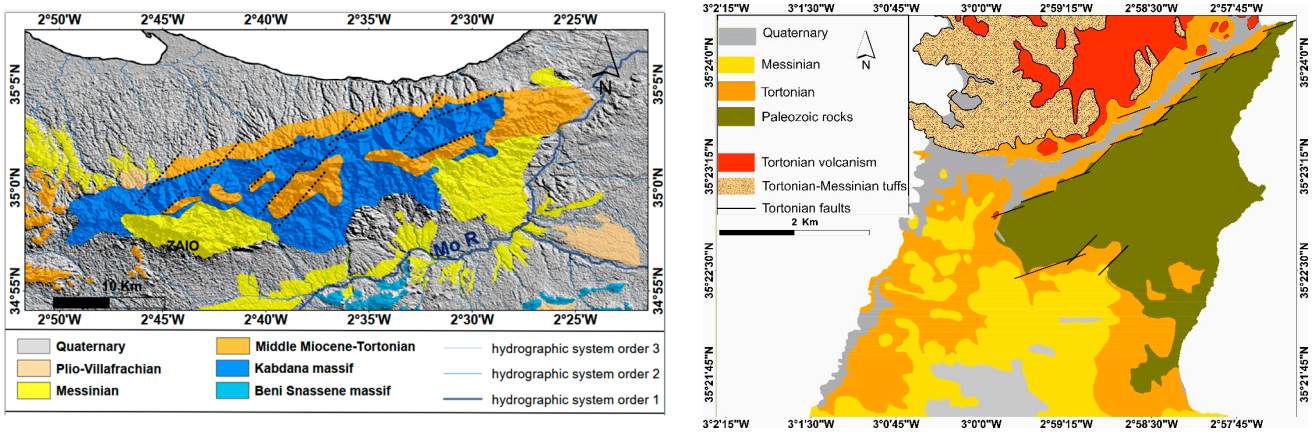

(**a**) (**b**)

Figure 10. Eastern Rif Tortonian key structures: (**a**) Kabdana Massif with faulted Tortonian deposits along the northern boundary; (**b**) Cap des Trois Fourches Massif, with faults affecting Tortonian deposits along the Palaeozoic boundary contacts.

4.2.2. Messinian Episode

The Eastern Rif post-nappe basins are also filled by Messinian formations that crop out with Plio-Quaternary thin deposits that locally cover them (Figure 2). These Messinian marly deposits evidence lineaments, which are relatively less expressed, variable in order

and extent, and often have a segmented appearance with orientations N120°E, N140°E, and N025°E (Figures 11, 12 and 13a). The Messinian deposits are predominantly crossed by a much dense and branched hydrographic network (Figure 11) that is oblique with respect to the previous main N70°E and N40°E hydrographic lineaments. Some of the N120°E lineaments extend over 10 km and outline the geometric boundaries of the Messinian outcrops, as is the case north of the Kert Basin (Twount sector) (Figure 12) and Ain Zora (Figure 13b).

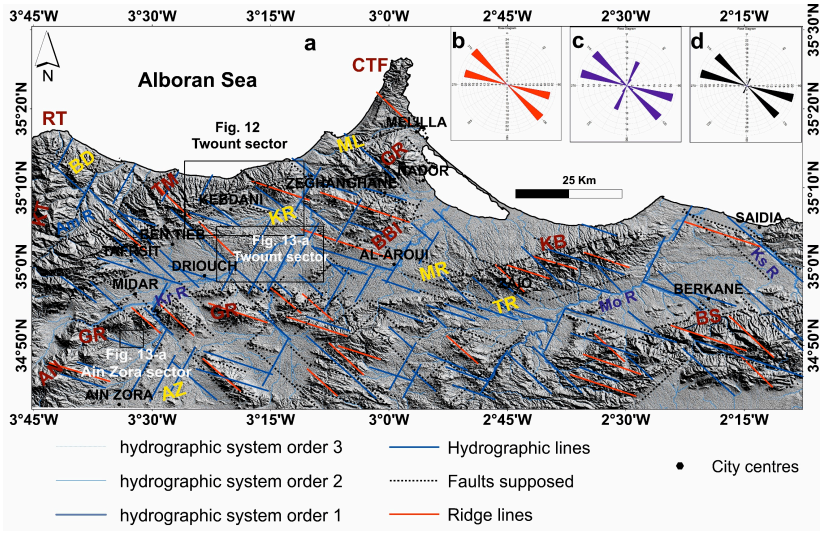

Figure 11. Lineament map showing the late structures that characterised the Messinian deformation system (**a**). Rose diagrams of the ridge lineaments (**b**), hydrographic lineaments (**c**), and supposed faults (**d**). Massifs: AN, Aknoul Nappe; AZ, Ain Zora; BBI, Beni Bou Ifroure; BS, Beni Snassene; CTF, Cap des Trois Fourches; GB, Gareb; GR, Gourougou; KB, Kabdana; KT, Ketama; RT, Ras Tarf; TM, Tamsamane. Basins: BD, Boudinar; KR, Kert; ML, Melilla; MR, Moulay Rachid; TR, Triffa. Hydrographic network: Am R, Amakran River; Ks R, Kiss River; Kt R, Kert River; MoR, Moulouya River.

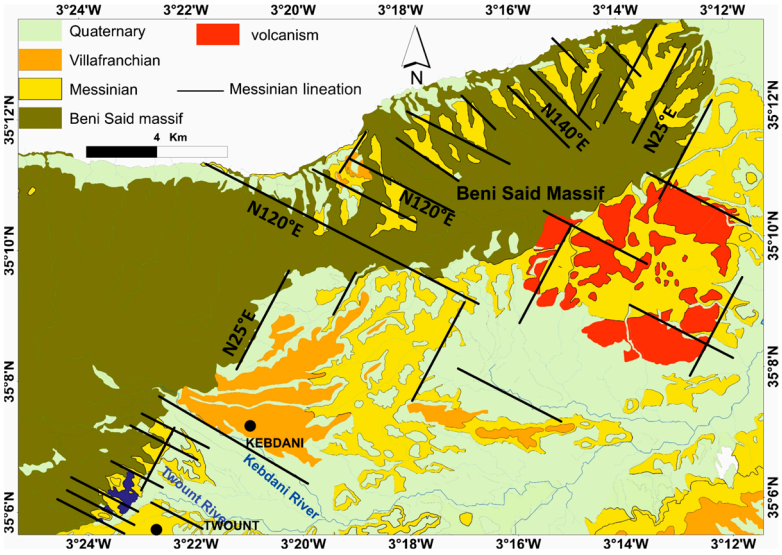

Figure 12. Messinian lineaments related to geological structures and Messinian deposits and unconformity on the metamorphic base of Beni Said Massif (modified from the Kebdani 1:50,000 scale geological map [23]).

Morphological examination shows that the hydrographic networks that cross the marly facies of the Messinian deposits are proportionally framed by ridge lineaments with little expression and with a larger radius of curvature than those of Tortonian deposits (Figure 8). This pattern is found in mountain ranges and in the same directions. Nevertheless, it is marked by a repetitive succession of raised ridge lineaments separated by these much embedded rivers. Some of these hydrographic networks extend over about ten kilometres and coincide with major structures that obliquely intersect all the mountain massifs and shift them according to dextral displacements.

Indeed, the cartographic examination shows that these Messinian formations have relatively different distributions of the underlying levels of the Tortonian. We note the local presence of some Messinian deposits that lie directly over the Jurassic and Cretaceous series of Beni Said and Kabdana massifs. These outcrops have well-defined geometric shapes, and their boundaries also strike N120°E, N140°E, and N025°E (Figure 9a,b). This geometry confirms the existence of an unconformity between the Messinian and Jurassic–Cretaceous basement. The contemporary activity of the structures that governed the development of the Messinian deposits is included in a distinct deformation stage, and their related brittle deformations obliquely intersect the regional faults of post-nappe basins attributed to the Tortonian (Figures 9 and 10). It is probably part of a shear zone system accommodated by regional N120°E dextral faults (Figure 13b).

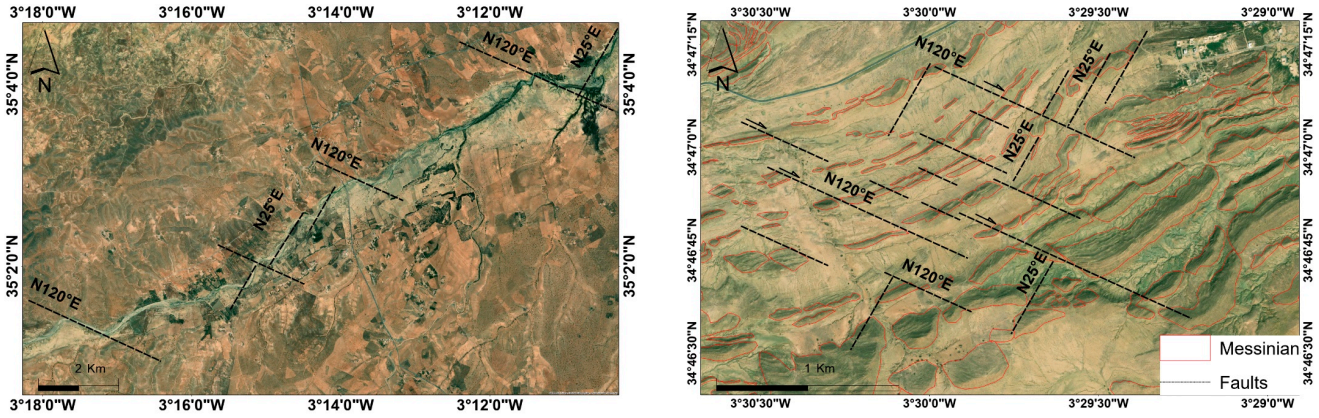

(**a**) (**b**)

Figure 13. Messinian lineaments: (**a**) satellite image showing N120°E structures intersecting with Oued Kert; (**b**) N120°E, N140°E, and N025°E faults deforming the bedding of Messinian formation at Ain Zora. Images from Google Earth (https://www.google.com/intl/es/earth/ accesed on 30 January 2024).

5. Discussion

Lineaments related to ridges, which coincide with the edges of massifs, and the hydrographic network have been presented in the Results section. They have preferent orientations and provide evidence of tectonic compartments and the presence of large fractures, including those related to folding. They may be interpreted in the frame of the geological evolution of the Eastern Rif since the Late Miocene. Two main episodes are differentiated: Tortonian and Messinian.

5.1. Tortonian Episode

The extension of these N70°E and N40°E faults is confirmed on a regional scale and coincides with the boundaries of formations attributed to the Upper Tortonian. This is evident in the olistostromic deposits found in the Kebdana and Ain Zora massifs [63–66], as well as the greenish marls that mark the N70°E fault along the northern edge of Kebdana [8,67]. Similarly, the Boudinar Basin is bounded to the south by the N45°E Nekor fault [8,12,13], whose activity determined the sedimentation during Tortonian [8,68]. Consequently, we can associate these structures with the first episode of Upper Miocene brittle deformations that controlled the regional morphostructural shaping of the Eastern Rif foreland.

These observations allow us to associate N40°E and N70°E structures with the first episode of brittle deformations of the Late Miocene that controlled the regional morphostructural shaping of the Eastern Rif foreland.

5.2. Messinian Episode

The regularity of the orientations of these lineaments can be considered the result of brittle deformations of variable order and extension that are in coherence with the scale of the Eastern Rif. Indeed, field data show that the geometry of the Messinian deposits, from the northwest edge of the Kert Basin (Twount area) above the Beni Said Massif (Figure 12) to the west of Melilla and the Ain Zora Basin level (Figure 13b) is controlled by N120°E long-term, dextral syn-sedimentary faults that are combined with sinistral N025°E faults. Faults of the same orientation have been described in the Messinian formations of the Boudinar Basin [17,50,69,70], as well as in the Lower Kert Basin [71].

5.3. Overprinting of Tortonian and Messinian Episodes: Evolution of the African Continental Margin

A NE-SW shortening of African–Eurasian lithospheric plates characterised the Middle Tortonian phase [72] that deforms the Western Mediterranean [69,73], where the Alboran Ridge (Figure 1) has NE-SW orientation similar to the Kabdana Massif. In this episode, the presence of N40°E and N70°E structures suggests an initial sinistral shear zone affecting the African margin.

The late N120°E dextral and N025°E sinistral structures characterising the Messinian episode may be correlated with the Yusuf Fault (N120°E dextral) of the Alboran Sea [73,74] and that of Al Idrissi (N025°E sinistral) [75–78].

These results highlight the interaction of tectonics and paleogeography during the opening and closing mechanisms of the South Rifian corridor. Indeed, the sedimentary basins of this corridor began to emerge since the Tortonian [14,17,79,80]. However, we found that the opening of this corridor is attributed to the Tortonian and may be related to the sinistral movement of the large N070°E faults. Their closure that caused the Messinian salinity crisis [17,19,50,81] should be controlled by the dextral movements of the N120°E faults.

The model shows that the Eastern Rif (Figure 14) underwent two deformation episodes during the Late Miocene. The first is characterised by a sinistral system driven by N70°E and N40°E faults. In the Western Mediterranean, these structures are represented in the Rif by the Jabha and Nekor faults [16,82,83] and in the Betic region by the Crevillente and Carboneras faults [82,84]. During the Tortonian, a sinistral movement towards the WSW is observed, and the sinistral slip of these faults is driven by a NE-SW-to-NNE-SSW compressive stress field [13]. The second episode shows a dextral deformation system mainly driven by N120°E combined with sinistral N25°E faults under NW-SE-to-NNW-SSE compression. These results confirm the deformation model observed in the Western Mediterranean [39,85–87].

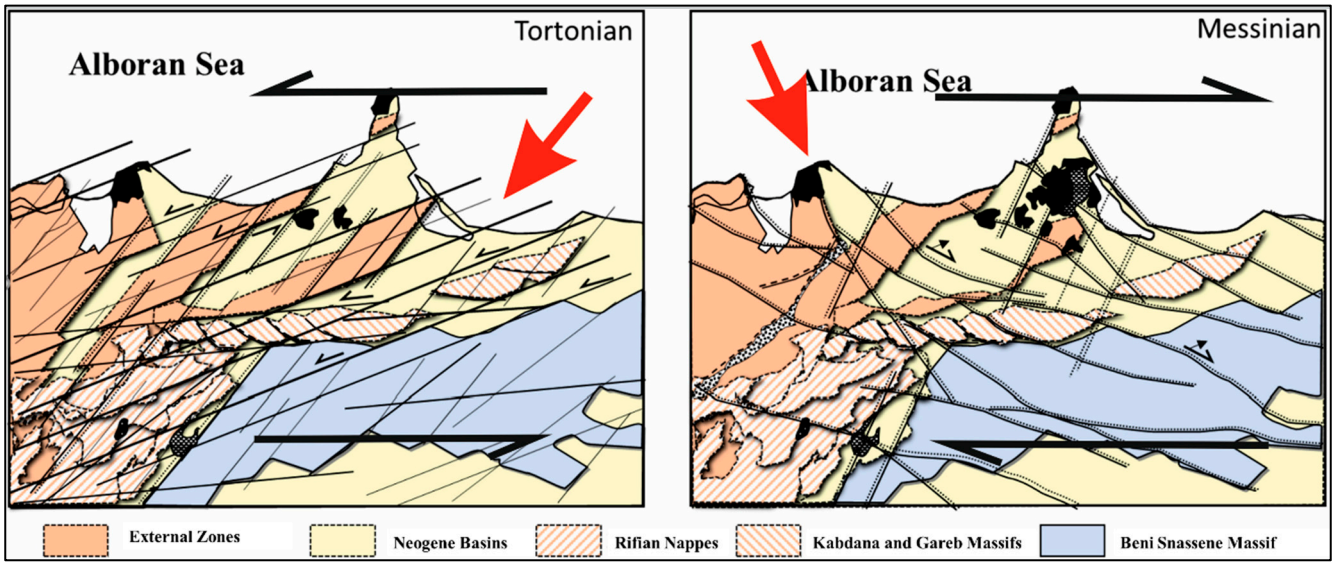

Figure 14. Deformation model of the Eastern Rif during the Tortonian and Messinian periods.

6. Conclusions

The analysis of the morphostructure of the Eastern Rif shows that the shaping of the reliefs is conditioned by the neotectonic deformation of the massive and rigid carbonate Jurassic and Cretaceous series controlled by well-developed Tortonian and Messinian structures that determined the crest lineaments. Hydrographic networks and coastlines follow incisions induced by regional structures that govern the individualisation of post-nappe basins. The ridge lineaments are related to fractures that individualised the pattern of the uplifted blocks and subsident basins. This multi-scale analytical study shows that these lineaments are organised according to two coherent deformation systems that characterise two neotectonic episodes.

The first episode (Tortonian) is at the origin of the major structures determined by the NE-SW-to-NNE-SSW compression developing regional N70°E and N40°E structures that generate the geometric pattern of rhomboid horst and graben shapes. The activity of these structures is part of a system of transtensive strike–slip fault deformations controlled by regional sinistral N70°E faults. The sedimentation of Late Tortonian deposits is established in an extensive context framed by N40°E faults. It is laterally compensated for mountainous areas by the N70°E and N110°E faults, which may correspond to transpressive zones.

The second episode (Messinian) is represented by tighter and smoother structures, which are mainly exposed in the unconformable Messinian deposits. Their geometry is mainly controlled by the NW-SE-to-NNW-SSE compression developing N120°E and N025°E faults, which are often combined with N140°E fractures. These faults intersect obliquely with previous structures and are part of a transtensive shearing deformation system controlled by N120°E dextral faults.

This study improves the knowledge of the post-nappe evolution of the Eastern Rif within the framework of the Western Mediterranean and constitutes a case study that highlights the suitability of morphotectonic analysis in regional areas affected by low, subtle deformations. The change from Tortonian to Messinian tectonic activity may have played a major role in closing the former Atlantic–Mediterranean connection, which finally contributed to the Messinian Salinity Crisis.

Author Contributions: Conceptualisation, M.M. and O.A.; methodology, M.M., O.A., K.B., V.T.-S. and J.G.-Z.; validation, M.M., O.A. and K.B.; formal analysis, M.M., O.A., K.B., V.T.-S. and J.G.-Z.; investigation, M.M., O.A., K.B., V.T.-S. and J.G.-Z.; resources, M.M., O.A. and J.G.-Z.; data curation, M.M., O.A. and K.B.; writing—original draft preparation, M.M., O.A., K.B., V.T.-S. and J.G.-Z.; writing—review and editing, M.M., O.A., K.B., V.T.-S. and J.G.-Z.; visualisation, M.M., O.A., K.B.,

V.T.-S. and J.G.-Z.; supervision, M.M., O.A., V.T.-S. and J.G.-Z. All authors have read and agreed to the published version of the manuscript.

Funding: This work was supported by the Applied Geosciences Laboratory, University of Oujda, Morocco, and the Spanish research group RNM 148 (Junta de Andalucia, Spain) and BARACA (PID2022-136678NB-I00 AEI/FEDER, UE) project.

Institutional Review Board Statement: Not applicable.

Informed Consent Statement: Not applicable.

Data Availability Statement: The original contributions presented in the study are included in the article, further inquiries can be directed to the corresponding author.

Conflicts of Interest: The authors declare no conflicts of interest.

References

1. Summerfield, M.A. Tectonic geomorphology. *Prog. Phys. Geogr.* **1991**, *15*, 193–205. [CrossRef]
2. Scheidegger, A.E. Global Morphotectonics. In *Morphotectonics*; Springer: Berlin, Germany, 2004. [CrossRef]
3. Gabrielsen, R.H.; Braathen, A. Models of fracture lineaments—Joint swarms, fracture corridors and faults in crystalline rocks, and their genetic relations. *Tectonophysics* **2014**, *628*, 26–44. [CrossRef]
4. Souei, A.; Zouaghi, T.; Khemiri, S. Lineament characterization for groundwater targeting using satellite images and field data. *Earth Sci. Inform.* **2023**, *16*, 455–479. [CrossRef]
5. Michard, A.; Chalouan, A.; Benyaich, A.; Samaka, F.; Dakki, M.; Bally, A.W.; Tejera de Leon, J.; Boutakiou, M.; Amar, A.; Ait Brahim, L.; et al. Observation et réponse: Commentaire sur la note: "Les bassins du Rif central (Maroc): Marqueurs de chevauchements hors-séquence d'âge miocène terminal au cœur de la chaîne". *Bull. Soc. Géol. Fr.* **1996**, *167*, 657–662.
6. Michard, A.; Goffé, B.; Bouybaouene, M.; Saddiqi, O. Late Hercynian–Mesozoic thinning in the Alboran domain: Metamorphic data from the northern Rif, Morocco. *Terra Nova* **1997**, *9*, 171–174. [CrossRef]
7. Negro, F.; Agard, P.; Goffé, B.; Saddiqui, O. Tectonic and metamorphic evolution of the Temsame units, External Rif (northern Morocco). Implications for the evolution of the Rif and the Betic-Rif arc. *J. Geol. Soc.* **2007**, *164*, 829–842. [CrossRef]
8. Azdimousa, A.; Jabaloy-Sánchez, A.; Münch, P.; Martínez-Martínez, J.M.; Booth-Rea, G.; Vázquez-Vílchez, M.; González-Lodeiro, F. Structure and exhumation of the Cap des Trois Fourches basement rocks (Eastern Rif, Morocco). *J. Afr. Earth Sci.* **2019**, *150*, 657–667. [CrossRef]
9. Rodríguez-Ruiz, M.D.; Abad, I.; Bentabol, M.; Cruz, M.D.R. Evidences of talc-white mica assemblage in low-grade metamorphic rocks from the internal zone of the Rif Cordillera (N Morocco). *Appl. Clay Sci.* **2020**, *195*, 105723. [CrossRef]
10. Chalouan, A.; Michard, A.; El Kadiri, K.; Negro, F.; Frizon de Lamotte, D.; Soto, J.I.; Saddiqi, O. The Rif Belt. In *Continental Evolution: The Geology of Morocco. Stratigraphy and Tectonics of the Africa-Atlantic-Mediterranean Triple Junction*; Lectures and Notes in Earth Sciences; Michard, A., Ed.; Springer: Berlin/Heidelberg, Germany, 2008; Volume 116, pp. 203–302.
11. Morel, J.L. Tectonique compressive au Messinien dans le Rif (Maroc). *C. R. Acad. Sci.* **1984**, *298*, 137–140.
12. Houzay, J.P. Géologie du Bassin de Boudinar (Rif Oriental, Maroc). Ph.D. Thesis, Université Paris-Sud, Orsay, France, 1975.
13. Aït Brahim, L. Tectoniques et États de Contrainte Récents du Maroc Nord. Résultats de la Cinématique des Plaques Afrique-Europe et du Bloc d'Alboran. Ph.D. Thesis, University Mohammed, V. Agdal Faculty of Sciences, Rabat, Morocco, 1991.
14. Azdimousa, A.; Bourgois, J. Les communications entre l'Atlantique et la Méditerranée par le couloir sud-rifain du Tortonien à l'Actuel: Stratigraphie séquentielle des bassins néogènes de la région du cap des Trois Fourches (Rif Oriental, Maroc). *J. Afr. Earth Sci.* **1993**, *17*, 975–980. [CrossRef]
15. Torbi, A.; Gélard, J.P. Paléocontraintes identifiées dans la couverture méso-cénozoïque du Maroc nord-oriental. Relations avec l'ouverture de l'Atlantique et le rapprochement Afrique–Europe. Comptes Rendus de l'Académie des Sciences. *Ser. IIA Earth Planet. Sci.* **2000**, *330*, 853–858. [CrossRef]
16. Galindo-Zaldívar, J.; Azzouz, O.; Chalouan, A.; Pedrera, A.; Ruano, P.; Ruiz-Constán, A.; Sanz de Galdeano, C.; Marín-Lechado, C.; Carlos López-Garrido, A.; Anahnah, F.; et al. Extensional tectonics, graben development and fault terminations in theeastern Rif (Bokoya–Ras Afraou area). *Tectonophysics* **2015**, *663*, 140–149. [CrossRef]
17. Achalhi, M.; Münch, P.; Cornée, J.J.; Azdimousa, A.; Melinte Dobrinescu, M.; Quillévéré, F.; Drinia, H.; Fauquette, S.; Jiménez-Moreno, G.; Merzeraud, G.; et al. The late Miocene Mediterranean-Atlantic connections through the north Rifian corridor: New insights from the Boudinar and Arbaa Taourirt basins (northeastern Rif, Morocco). *Palaeogeogr. Palaeoclimatol. Palaeoecol.* **2016**, *459*, 131–152. [CrossRef]
18. Iribarren, L.; Vergés, J.; Fernàndez, M. Sediment supply from the Betic–Rif orogen to basins through Neogene. *Tectonophysics* **2009**, *475*, 68–84. [CrossRef]
19. Krijgsman, W.; Langereis, C.G.; Zachariasse, W.J.; Boccaletti, M.; Moratti, G.; Gelati, R.; Iaccarino, S.; Papani, G.; Villa, G. Late Neogene evolution of the Taza–Guercif Basin (Rifian Corridor, Morocco) and implications for the Messinian salinity crisis. *Mar. Geol.* **1999**, *153*, 147–160. [CrossRef]
20. Faure-Muret, A. Carte géologique du Maroc au 1/50,000, feuille de Nador. Notes Mém. Serv. Géol. 2002, Maroc, n° 379.

21. Guillemin, M.; Hernandez, J.; Wildi, W. Carte géologique du Maroc au 1/50,000, feuille de Melilla. Notes Mém. Serv. Géol. 1983, Maroc, n° 297.
22. Faure-Muret, A. Carte géologique du Maroc au 1/50,000, feuille de Zeghanghane. Notes Mém. Serv. Géol. 1996, Maroc, n° 370.
23. Choubert, G.; Faure-Muret, A. Carte géologique du Maroc au 1/50,000, feuille de Kebdani. Notes Mém. Serv. Géol. 1984, Maroc, n° 301.
24. Choubert, G.; Faure-Muret, A. Carte géologique du Maroc au 1/50,000, feuille de Boudinar. Notes Mém. Serv. Géol. 1984, Maroc, n° 299.
25. Faure-Muret, A.; Choubert, G.; Morel, J.L.; De Lamotte, F.; Darraz, C. Carte géologique du Maroc au 1/50,000, feuille de Midar. Notes Mém. Serv. Géol. 1994, Maroc, n° 367.
26. Leblanc, D.; Feinberg, H.; Lorenz, H.G.; Wernli, R.; Septfontaine, M. Carte géologique du Maroc au 1/50,000, feuille d'Ain Zohra. Notes Mém. Serv. Géol. 1996, Maroc, n° 371.
27. Chaieb, M.; Boudchiche, L.; Guardia, P. Carte géologique du Maroc au 1/50,000, feuille d'Ahfir. Notes Mém. Serv. Géol. 2004, Maroc, n° 453.
28. Domingo, A.G.; Arias, A.M. Carte géologique du Maroc au 1/50,000, feuille de Berkane. Notes Mém. Serv. Géol. 2001, Maroc, n° 425.
29. Domingo, A.G.; Arias, A.M. Carte géologique du Maroc au 1/50,000, feuille de Zaio. Notes Mém. Serv. Géol. 2001, Maroc, n° 425.
30. Ennadifi, M.Y.; Hamel, C. Carte géologique du Maroc au 1/100,000, feuille de Tistoutine. Notes Mém. Serv. Géol. 1971, Maroc, n° 167.
31. Choubert, G.; Marçais, J.; Suter, G. Carte géologique du Maroc au 1/500,000, feuille de Oujda. Notes Mém. Serv. Géol. 1956, Maroc, n° 70.
32. Suter, G. Carte structurale du Maroc au 1/500,000, feuille de Rif. Notes Mém. Serv. Géol. 1980, Maroc.
33. Durand-Delga, M. *La Courbure de Gibraltar, Extrémité Occidentale des Chaînes Alpines, Unit l'Europe et l'Afrique*; Birkhäuser: Basel, Switzerland, 1972.
34. Kornprobst, J. Contribution à l'étude pétrographique et structurale de la zone interne du Rif (Maroc septentrional). *Notes Mém. Serv. Géol. Maroc.* **1974**, *251*, 256.
35. Sanz de Galdeano, C. Paleogeographic reconstruction of the Betic-Rif Internal Zone: An attempt. *Rev. Soc. Geol. España* **2019**, *32*, 107–128.
36. Bouillin, J.P.; Durand-Delga, M.; Gelard, J.P.; Leikine, M.; Raoult, J.F.; Raymont, D.; Tefiani, M.; Vila, J.M. Définition d'un flysch massylien et d'un flysch mauréta-nien au sein des flyschs allochtones de l'Algérie. *CR Ac. Sc. Paris* **1970**, *298*, 655–660.
37. Raoult, J.F. *Géologie du Centre de la Chaine Numidique (Nord du Constantinois, Algérie)*; Société Géologique de France: Orleans, France, 1974.
38. El Talibi, H.; Zaghloul, M.N.; Perri, F.; Aboumaria, K.; Rossi, A. Sedimentary evolution of the siliciclastic Aptian–Albian Massylian flysch of the Chouamat Nappe (central Rif, Morocco). *J. Afr. Earth Sci.* **2014**, *100*, 554–568. [CrossRef]
39. Gimeno-Vives, O.; De Lamotte, D.F.; Leprêtre, R.; Haissen, F.; Atouabatc, A.; Mohn, G. The structure of the Central-Eastern External Rif (Morocco); Poly-phased deformation and role of the under-thrusting of the North-West African paleo-margin. *Earth Sci. Rev.* **2020**, *205*, 103198. [CrossRef]
40. De Luca, P. L'unite chaoutique des Kabdana (région de Zaio, Maroc). Relation structurale avec l'avant-pays du Rif oriental. *Bull. Soc. Géol. France P.* **1978**, *3*, 339–343. [CrossRef]
41. Kerchaoui, S. Etude Géologique et Structurale du Masifdes Beni Bou Ifrour (Rif Oriental, Maroc). Ph.D. Thesis, Université de Paris-Sud, Paris, France, 1985. Volume 11.
42. Makkaoui, M.; Azzouz, O.; Belhaj, K.; Moqaddem, A. Lithostratigraphic analysis and characterization of the upper miocene deformation of the Beni Bou Ifroure massif (Jbel Harcha Unit) eastern Rif Morocco. *EDP Sci.* **2023**, *364*, 01011. [CrossRef]
43. Hoepffner, C. La Tectonique Hercynienne dans l'Est du Maroc. Ph.D. Thesis, Université Louis Pasteur, Strasbourg, France, 1987.
44. Oujidi, M. Complexe Volcano-Sédimentaire Rouge du Trias et de la Base du Lias des 458 Pays des Horsts (Maroc Oriental). Ph.D. Thesis, Mohammed First University, Oujda, Morocco, 1994, unpublished work.
45. Oujidi, M.; Elmi, S. Architectural evolution of the Oujda Mountains (eastern 460 Morocco) during the Triassic and the early Jurassic. *Bull. Soc. Geol. Fr.* **2000**, *171*, 169–179. [CrossRef]
46. Leblanc, M.; Lancelot, J.R. Interprétation géodynamique du domaine pan-africain (Précambrien terminal) de l'Anti-Atlas (Maroc) à partir de données géologiques et géochronologiques. *Can. J. Earth Sci.* **1980**, *17*, 142–155. [CrossRef]
47. De Lamotte, F. La structure du Rif oriental (Maroc). *Mém. Sc. Terre Univer. P. M. Curie Paris VI* **1985**, *15*, 436.
48. Guillemin, M.; Houzay, J.P. Le Néogène post-nappes et le Quaternaire du Rif Nord oriental. Stratigraphie et tectonique des bassins de Melilla, de Kert, de Boudinar et du piémont des Kabdana. *Notes Mém. Serv. Géol. Maroc.* **1982**, *314*, 7–239.
49. De Lamotte, D.F. Contribution à l'Étude de l'Évolution Structurale du Rif Oriental (Maroc). Ph.D. Thesis, Université Paris-Sud, Paris, France, 1979.
50. Azdimousa, A.; Poupeau, G.; Rezqi, H.; Asebry, L.; Bourgois, J.; Ait Brahim, L. Géodynamique des bordures méridionales de la mer d'Alboran; application de la stratigraphie séquentielle dans le bassin néogène de Boudinar (Rif oriental, Maroc) 28. *Bull. Inst. Sci. Rabat* **2006**, *28*, 9–18.
51. Suter, G.; Fiechter, G.G. Le Rif méridional atlantique (Maroc): Aperçu structural sur la région de Zoumi-Ouezzane et le pays du Habt (Larache). *Notes Mém. Serv. Géol. Rabat* **1966**, *26*, 15–20.
52. Frizon de Lamotte, D. Contribution à l'Étude de l'Tévolution Structural du Rif Oriental (Maroc). Ph.D. Thesis, Universite de Paris XI, Orsay, France, 1979.

53. Azdimousa, A.; Jabaloy, A.; Asebriy, L.; Booth-Rea, G.; González-Lodeiro, F.; Bourgois, J. Lithostratigraphy and structure of the Temsamane unit (eastern external Rif, Morocco). *Rev. Soc. Geoll España* **2007**, *20*, 187–200.
54. Michard, A.; Hœpffner, C.; Soulaimani, A.; Baidder, L. The Variscan Belt. In *Continental Evolution: The Geology of Morocco: Structure, Stratigraphy, and Tectonics of the Africa-Atlantic-Mediterranean Triple Junction*; Springer: Berlin/Heidelberg, Germany, 2008; pp. 65–132.
55. Booth-Rea, G.; Jabaloy-Sánchez, A.; Azdimousa, A.; Asebriy, L.; Vázquez Vílchez, M.; Martínez-Martínez, J.M. Upper-crustal extension during oblique collision: The Temsamane extensional detachment (eastern Rif, Morocco). *Terra Nova* **2012**, *24*, 505–512. [CrossRef]
56. Kouamé, K.F.; Penven, M.J.; Kouadio, B.H.; Saley, M.H.; Gronayes, C.C. Contribution des images d'aster de terra et D'un modèle numérique d'altitude à la cartographie morpho structurale du masifdes Toura (Ouest de la Côte d'Ivoire). *Télédétection* **2006**, *6*, 103–121.
57. Youan, T.A.M.; Lasm, T.; Jourda, J.P.; Kouame, K.F.; Razack, M. Cartographie structurale par imagerie satellitaire ETM+ de Landsat-7 et analyse des réseaux de fractures du socle précambrien de la région de Bondoukou (Nord-Est de la Côte d'Ivoire). *Rev. Télédétect.* **2008**, *8*, 119–135.
58. Abdou Babaye, M.S. Evaluation des Ressources en Eau Souterraine dans le Bassin de Dargol (Liptako-Niger). Ph.D. Thesis, Université de Liège, Liege, Belgium, 2012.
59. Mallast, U.; Gloaguen, R.; Geyer, S.; Rodiger, T.; Siebert, C. Derivation of groundwater flow-paths based on semi-automatic extraction of lineaments from remote sensing data. *Hydrol. Earth Syst. Sci.* **2011**, *15*, 2665–2678. [CrossRef]
60. Šilhavý, J.; Minár, J.; Mentlík, P.; Sládek, J. A new artefacts resistant method for automatic lineament extraction using Multi-Hillshade Hierarchic Clustering (MHHC). *Comput. Geosci.* **2016**, *92*, 9–20. [CrossRef]
61. Khattach, D.; Keating, P.; Chennouf, T.; Andrieux, P.; Milhi, A. Apport de la gravimétrie à l'étude de la structure du bassin des Triffa (Maroc nord-oriental): Implications hydrogéologiques. *C. R. Geosci.* **2004**, *336*, 1427–1432. [CrossRef]
62. Khattach, D.; Mraoui, H.; Sbibih, D.; Chennouf, T. Analyse multi-échelle par ondelettes des contacts géologiques: Application à la carte gravimétrique du Maroc nord-oriental. *C. R. Geosci.* **2006**, *338*, 521–526. [CrossRef]
63. Rampnoux, J.P.; Angelier, J.; Colletta, B.; Fudral, S.; Guillemin, M.; Pierre, G. Sur l'Évolution Néotectonique du Maroc Septentrional. *Géologie Méditerranéenne* **1979**, *6*, 439–464. [CrossRef]
64. Bourgois, J. D'une étape géodynamique majeure dans la genèse de l'arc de Gibraltar: "L'hispanisation des flyschs rifains au Miocène inférieur". *Bull. Soc. Géol. Fr.* **1977**, *19*, 1115–1119. [CrossRef]
65. Kerzazi, K. Etude Biostratigraphique du Miocène sur la Base des Foraminifères Planctoniques et Nannofossiles Calcaires dans le Prérif et la Marge atlantique du Maroc (site 547A du DSDP Leg 79), Aperçu sur Leur Paléoenvironnement. Ph.D. Thesis, Sorbonne Université, Paris, France, 1994. Volume 6.
66. Morel, J.L. Etats de contrainte et cinématique de la chaîne rifaine (Maroc) du Tortonien à l'actuel. *Geodin. Acta* **1989**, *3*, 283–294. [CrossRef]
67. Hervouet, Y.; De Luca, P. Place de l'unite chaotique de Gareb-Kabdana dans 434 l'orogene rifain; implications geodynamiques. *Bull. Soc. Geol. Fr.* **1980**, *435*, 305–310. [CrossRef]
68. Poujol, A.; Ritz, J.F.; Tahayt, A.; Vernant, P.; Condomines, M.; Blard, P.H.; Billant, J.; Vacher, L.; Tibari, B.; Hni, L.; et al. Active tectonics of the Northern Rif (Morocco) from geomorphic and geochronological data. *J. Geodyn.* **2014**, *77*, 70–88. [CrossRef]
69. Lafosse, M.; D'Acremont, E.; Rabaute, A.; Estrada, F.; Jollivet-Castelot, M.; Vazquez, J.T.; Galindo-Zaldivar, J.; Ercilla, G.; Alonso, B.; Smit, J.; et al. Plio-Quaternary tectonic evolution of the southern margin of the Alboran Basin (Western Mediterranean). *Solid Earth* **2020**, *11*, 741–765. [CrossRef]
70. Lafosse, M.; Gorini, C.; Le Roy, P.; Alonso, B.; d'Acremont, E.; Ercilla, G.; Rabineau, M.; Vázquez, J.T.; Rabaute, A.; Ammar, A. Late Pleistocene-Holocene history of a tectonically active segment of the continental margin (Nekor basin, Western Mediterranean, Morocco). *Mar. Pet. Geol.* **2018**, *97*, 370–389. [CrossRef]
71. Nasri, H. Caractérisations Minéralogique, Géochimique, Sédimentologique et Géotechnique des Argiles Néogènes du Rif Nord Oriental du Maroc en Vue de Leur Valorisation dans l'Industrie Céramique. Ph.D. Thesis, University of Liège, Liege, Belgium, 2019.
72. Brahim, L.A.; Chotin, P.; Hinaj, S.; Abdelouafi, A.; El Adraoui, A.; Nakcha, C.; Dhont, D.; Charroud, M.; Alaoui, F.S.; Amrhar, M.; et al. Paleostress evolution in the Moroccan African margin from Triassic to Present. *Tectonophysics* **2002**, *357*, 187–205. [CrossRef]
73. Koulali, A.; Ouazar, D.; Tahayt, A.; King, R.W.; Vernant, P.; Reilinger, R.E.; McClusky, S.; Mourabit, T.; Davila, J.M.; Amraoui, N. New GPS constraints on active deformation along the Africa–Iberia plate boundary. *Earth Planet. Sci. Lett.* **2011**, *308*, 211–217. [CrossRef]
74. Perea, H.; Gràcia, E.; Almeida, S.; Gómez de la Peña, L.; Martínez-Loriente, S.; Bartolomé, R. Revealing the earthquake history during the last 200 ka on a large submarine strike-slip fault: The Yusuf Fault System (Alboran Sea). In Proceedings of the 22nd EGU General Assembly, Online, 4–8 May 2020.
75. D'Acremont, E.; Gutscher, M.A.; Rabaute, A.; de Lépinay, B.M.; Lafosse, M.; Poort, J.; Gorini, C. High-resolution imagery of active faulting offshore Al Hoceima, Northern Morocco. *Tectonophysics* **2014**, *632*, 160–166. [CrossRef]
76. Lafosse, M.; d'Acremont, E.; Rabaute, A.; Mercier de Lépinay, B.; Tahayt, A.; Ammar, A.; Gorini, C. Evidence of quaternary transtensional tectonics in the Nekor basin (NE Morocco). *Basin Res.* **2016**, *29*, 470–489. [CrossRef]

77. Gràcia, E.; Grevemeyer, I.; Bartolomé, R.; Perea, H.; Martínez-Loriente, S.; Gómez de la Peña, L.; Villaseñor, A.; Klinger, Y.; Lo Iacono, C.; Diez, S.; et al. Earthquake crisis unveils the growth of an incipient continental fault system. *Nat. Commun.* **2019**, *10*, 3482. [CrossRef]
78. Tendero-Salmerón, V.; Lafosse, M.; D'acremont, E.; Rabaute, A.; Azzouz, O.; Ercilla, G.; Makkaoui, M.; Galindo-Zaldivar, J. Application of automated throw backstripping method to characterize recent faulting activity migration in the Al Hoceima Bay (Northeast Morocco): Geodynamic implications. *Front. Earth Sci.* **2021**, *9*, 645942. [CrossRef]
79. Pratt, J.R.; Barbeau, J.D.L.; Izykowski, T.M.; Garver, J.I.; Emran, A. Sedimentary provenance of the Taza-Guercif basin, south Rifean Corridor, Morocco: Implications for basin emergence. *Geosphere* **2016**, *12*, 221–236. [CrossRef]
80. Bernini, M.; Boccaletti, M.; Gelati, R.; Moratti, G.; Papani, G.; Mokhtari, J.E. Tectonics and sedimentation in the Taza-Guercif Basin, Northern Morocco: Implications for the Neogene Evolution of the Rif-Middle Atlas Orogenic system. *J. Pet. Geol.* **1999**, *22*, 115–128. [CrossRef]
81. Gorini, C.; Montadert, L.; Rabineau, M. New imaging of the salinity crisis: Dual Messinian lowstand megasequences recorded in the deep basin of both the eastern and western Mediterranean. *Mar. Pet. Geol.* **2015**, *66*, 278–294. [CrossRef]
82. Leblanc, D.; Olivier, P. Role of strike-slip faults in the Betic-Rifian orogeny. *Tectonophysics* **1984**, *101*, 345–355. [CrossRef]
83. Benmakhlouf, M.; Galindo-Zaldívar, J.; Chalouan, A.; de Galdeano, C.S.; López-Garrido, A.C. Inversion of transfer faults: The Jebha–Chrafate fault (Rif, Morocco). *J. Afr. Earth Sci.* **2012**, *73*, 33–43. [CrossRef]
84. Meijninger, B.M.L.; Vissers, R.L.M. Miocene extensional basin development in the Betic Cordillera, SE Spain revealed through analysis of the Alhama de Murcia and Crevillente Faults. *Basin Res.* **2006**, *18*, 547–571. [CrossRef]
85. Estrada, F.; Galindo-Zaldívar, J.; Vázquez, J.T.; Ercilla, G.; d'Acremont, E.; Alonso, B.; Gorini, C. Tectonic indentation in the central Alboran Sea (westernmost Mediterranean). *Terra Nova* **2018**, *30*, 24–33. [CrossRef]
86. Tendero-Salmerón, V.; Galindo-Zaldivar, J.; D'Acremont, E.; Catalán, M.; Martos, Y.M.; Ammar, A.; Ercilla, G. New insights on the Alboran Sea basin extension and continental collision from magnetic anomalies related to magmatism (western Mediterranean). *Mar. Geol.* **2022**, *443*, 106696. [CrossRef]
87. Abbassi, A.; Cipollari, P.; Zaghloul, M.N.; Cosentino, D. The Rif chain (northern Morocco) in the late Tortonian-early Messinian tectonics of the Western Mediterranean orogenic belt: Evidence from the Tanger-Al Manzla wedge-top basin. *Tectonics* **2020**, *39*, e2020TC006164. [CrossRef]